

Study on the inhibition of hyperthermic CO₂ pneumoperitoneum on the proliferation and migration of colon cancer cells and its mechanism

JIAYING ZHAO^{1*}, YUANKUN CAI^{1*}, CHENQING YIN¹, YOU LV¹, WANMIN WEI², XIN WANG¹, ZONG HAO¹, CHENXIA SHEN¹, HUIPENG WANG¹ and JUN CHEN¹

¹Department of General Surgery and ²Central Laboratory, The Fifth People's Hospital of Shanghai, Fudan University, Shanghai 200240, P.R. China

Received September 18, 2015; Accepted October 26, 2015

DOI: 10.3892/or.2015.4446

Abstract. The present study explored the inhibitory effect of hyperthermic CO₂ pneumoperitoneum on the proliferation and migration of colon cancer cells, and its mechanism. Colon cancer cell line SW-480 was sealed into a urine collection bag to simulate pneumoperitoneum with 100% CO₂ under a pressure of 14 mmHg. The growth and morphology of cells were observed under a microscope, the inhibition on cell proliferation was measured using WST-8 test, cell apoptosis and the cell cycle were monitored using fluorescence-activated cell sorting analysis, the migration of cells was tested using the scratch assay, and the expression of HSP-70, caspase-3, hypoxia-inducible factor-1 α (HIF-1 α) and matrix metalloproteinase-9 (MMP-9) proteins and genes was investigated using western blotting and reverse transcription polymerase chain reaction. Compared with the control group, there was no significant difference in the CO₂ group ($P > 0.05$), while the apoptosis and necrosis rates in the hyperthermo-CO₂ group was significantly increased ($P < 0.05$). Compared with the control group, the number of cells at G0/G1 phase significantly increased and the number of cells at S phase significantly decreased in the hyperthermo-CO₂ group ($P < 0.05$), indicating that hyperthermo-CO₂ could arrest the cell cycle. It was suggested by the results of the scratch assay that cell migration ability enhanced in the CO₂ group, but decreased in the hyperthermo-CO₂ group compared with the control. CO₂ pneumoperitoneum promoted cell migration by upregulating HIF-1 α and MMP-9 expression. However, the CO₂ pneumoperitoneum with hyperthermia enhanced apoptosis and inhibited migration by

upregulating the expression of HSP-70, HIF-1 α and caspase-3, but downregulating the expression of MMP-9.

Introduction

Laparoscopic technology has been widely adopted in colorectal surgery and CO₂ is commonly used to create laparoscopic pneumoperitoneum. However, the effect of CO₂ pneumoperitoneum on tumor proliferation and metastasis is still controversial. Various researchers believed that the therapeutic effect of laparoscopic colon cancer surgery under CO₂ pneumoperitoneum was equivalent to that of conventional laparotomy, increasing neither the recurrence rate nor the local or remote metastasis rate (1). However, a majority of them considered that CO₂ pneumoperitoneum could promote colon cancer cell proliferation or metastasis under persistent pressure for a certain time period (2-4). Intraperitoneal hyperthermia chemoperfusion (IHCP) was reported to effectively eliminate tumor cells and small tumor metastasis in the peritoneal cavity, and prevent tumor peritoneal dissemination (5,6), which has been utilized as adjuvant therapy after open surgeries on gastric, colorectal and ovarian cancer. However, it is still an open question how to reduce the adverse effect of CO₂ pneumoperitoneum on the therapeutic effect of colon cancer surgery, and how to utilize IHCP as combined therapy. It has been speculated that the therapeutic effect may be improved by introducing heated CO₂ into the abdomen simulating IHCP at 43°C before laparoscopic therapy. In the present study, the *in vitro* assay was used to investigate the effect of CO₂ pneumoperitoneum with hyperthermia on colon cancer cell proliferation and metastasis.

Materials and methods

Cell culture. Colon cell line SW-480 was provided by Shanghai Cell Bank of Chinese Academy of Sciences (Shanghai, China) and was cultured with L-15 medium (pH 7.35) containing 10% calf serum in an incubator at 37°C supplemented with 5% CO₂, 20% O₂ and 75% N₂. The culture medium was refreshed every other day, and the cells at logarithmic growth phase were used for the experiment.

Correspondence to: Dr Jiaying Zhao, Department of General Surgery, The Fifth People's Hospital of Shanghai, Fudan University, Shanghai 200240, P.R. China
E-mail: zhaojiaying001@126.com

*Contributed equally

Key words: carbon dioxide pneumoperitoneum with hyperthermia, colon cancer cell line, migration, proliferation

Materials and instruments. L-15 culture medium was purchased from Gibco (Thermo Fisher Scientific, San Jose, CA, USA), and calf serum was obtained from Hangzhou Tianhang Biological Technology Co., Ltd. (Hangzhou, China). The following reagents or kits were used: CCK-8 cytotoxicity analysis kit, Annexin V-FITC apoptosis detection kit (both from Dojindo Laboratories, Japan), KGI cell DNA content detection kit, TRIzol reagent (Invitrogen, USA), RNA extraction kit-RNAiso Plus (Takara, Japan), First Strand cDNA Synthesis kit and Maxima SYBR-Green/ROX qPCR Master mix (both from Thermo Fisher Scientific). The first antibodies were procured from Abcam (USA), including mouse monoclonal antibody against HSP-70 or HIF-1 α and rabbit monoclonal antibody against Matrix metalloproteinase-9 (MMP-9) or caspase-3. The secondary antibodies were procured from Arigo, including goat anti-rabbit IgG and goat anti-mouse IgG. Polymerase chain reaction (PCR) primers were designed and synthesized by Sangon Biotech (Shanghai, China). The equipment included the ELISA reader (Thermo, USA), flow cytometry (BD FACSCalibur; USA), western blot electrophoresis (Bio-Rad, USA) and fluorescent-PCR machine (Applied Biosystems, USA).

Cell treatment and experimental grouping. The disposable 2-L urine collection bag was utilized to simulate the pneumoperitoneum. A small cut was made on the lateral part of the urine collection bag, through which a balanced plate was inserted and the Petri dish or 96-well plate was attached. The cut was then sealed using the sealer. One port of the urine collection bag was connected with 100% CO₂, while the other port was connected to blood-pressure meter to monitor the pressure of CO₂ with the preset of 14 mmHg. The temperature was set at 43 and 37°C, using a cell culture incubator for 2 h. The cells were divided into the control, the CO₂ pneumoperitoneum and the hyperthermo-CO₂ pneumoperitoneum group, and then put back into the normal incubator.

Proliferation and morphology of cells. The cells were seeded onto the six-well plate at a density of 5x10⁵/well in 2 ml. The cells from each group were observed and photographed under the microscope at 12, 24, 36, 48, 60 and 72 h after the treatment. The experiment was repeated three times.

Cell proliferation inhibition detection using the WST-8 test. The cells of 1x10⁴/well at logarithmic growth phase were seeded onto the 96-well plate and cultured for 24 h. Then the cells from each group were separately treated with continued culturing for 12, 24, 36, 48, 60 and 72 h. CCK-8 (10 μ l) was added to each well for 4 h in the absence of light. The optical density (OD) value at 450 nm was measured to represent the number of viable cells after subtracting the OD value from the OD value of phosphate-buffered saline (PBS). The triplicate wells were used for average calculation, and the cell proliferation inhibition was calculated to plot the curve of proliferation inhibition, using the formula: Cell proliferation inhibition rate = 1 - (OD of treated group - OD of background)/(OD of control group - OD of background) x 100%.

Cell apoptosis and necrosis detection using fluorescence-activated cell sorting analysis. The cells were seeded onto the

six-well plate at a density of 5x10⁵/well in 2 ml and cultured for 24 h. Then, the cells were separately treated and collected after another 12 h of normal culture. The cells were resuspended in 1X binding buffer after washing twice with cold PBS, and adjusted to the density of 1x10⁶/ml. Cell suspensions (100 μ l) were transferred to a 5-ml tube for fluorescence-activated cell sorting (FACS). Annexin V-FITC and propidium iodide (PI), 5 μ l each, were added into the cell suspensions and incubated for 15 min at room temperature in the absence of light. The cell mixture was incubated on ice after adding 400 μ l of 1X binding buffer, and FACS analysis was performed within 1 h. FITC/PI⁻ was defined as normal cells, FITC⁺/PI⁻ was defined as apoptotic cells at an early stage, FITC⁺/PI⁺ was defined as apoptotic cells at a late stage, and FITC⁻/PI⁺ was defined as necrotic cells. The experiment was repeated three times. The apoptotic index (AI) and necrotic rate were calculated using the averaged measurements from the experiments. AI = (number of apoptotic cells at late stage + number of apoptotic cells at early stage)/total number of cells; necrotic rate = number of necrotic cells/total number of cells.

Cell cycle detection using FACS. Cells (1x10⁶/ml) were collected and washed twice with ice-cold PBS. Then the cells were fixed in 70% precooled ethanol overnight. The fixation buffer was discarded, RNAase (0.1 mg/ml) was added into the cells after washing twice with PBS, and the cells were incubated at 37°C for 30 min. Then, 1 ml of PI (50 mg/l) was added and incubated for 30 min before FACS analysis. The experiments were repeated three times.

Extracellular fluid temperature and pH measurements. The temperature and pH of the culture medium from each group were measured using a thermometer and a pH probe.

Cell scratch test. We used the scratch test to detect the migration of the cells, since SW-480 cells showed adherent growth. The cells at logarithmic growth phase were seeded onto the six-well plate at a density of 5x10⁵/well in 2 ml and cultured for 48 h. The normal culture was continued for 24 h after the treatment of each group. A straight line was scratched onto the bottom of Petri dish using a syringe needle, and the cell proliferation and crossing line were observed under the microscope at 24, 36, 48, 60 and 72 h.

Expression of protein detection using western blotting. The cells were continuously cultured for 2 or 12 h after the treatment, and 1x10⁷ cells were collected. Radioimmunoprecipitation assay lysis buffer (150 μ l) was added, and the supernatants were used for total protein determination; the protein concentration ranged between 1.5 and 2.5 mg/ml. The supernatants were aliquoted into 20 μ l x2 and stored at -80°C. Sodium dodecyl sulfate (SDS)-polyacrylamide separating (10%) and concentrating gels (6%) were prepared; 80 μ g proteins from each group were mixed with 5X SDS loading buffer and subjected to SDS-polyacrylamide gel electrophoresis (PAGE) after denaturing at 100°C for 10 min. The PAGE was stopped according to the migration of the dye and protein markers, and the proteins were then transferred to the polyvinylidene fluoride (PVDF) membrane. The first antibody was incubated with PVDF membrane overnight after blocking with skimmed

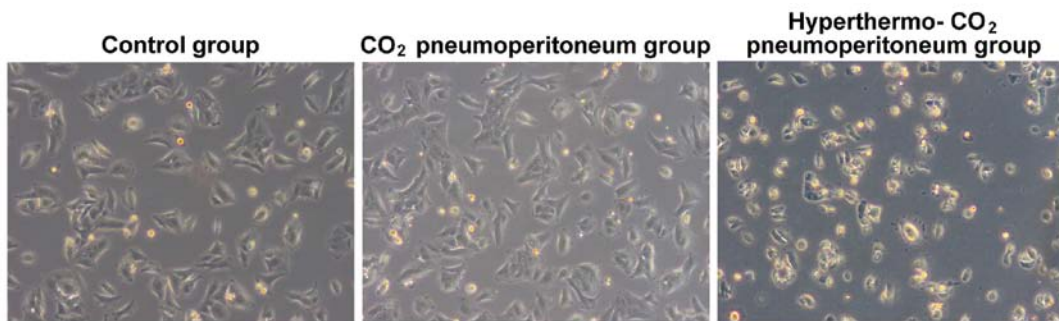


Figure 1. The morphology of each group after treatment for 24 h.

milk solution for 1 h, and the secondary antibody was incubated for 1 h at room temperature before enhanced chemiluminescence developing and photographing. The molecular weight of the targeted protein was estimated using protein markers, and β -actin was adopted as the internal control to evaluate the total amount of protein-loaded onto each lane. The images were analyzed using ImageJ software; the amount of the targeted protein = relative gray scale \times area (mm^2). The expression levels of HSP-70, caspase-3, hypoxia-inducible factor-1 α (HIF-1 α) and MMP-9 were separately calculated for comparison.

Fluorescence quantitative PCR. The relative mRNA amounts of HSP-70, caspase-3, HIF-1 α and MMP-9 were detected using fluorescence quantitative PCR. The cells were collected after each treatment, the total RNA was extracted using TRIzol reagent and cDNA was synthesized using a First Strand cDNA Synthesis kit (MD, USA). The primers were designed and synthesized by Sango Biotech as follows: HSP-70 forward, TA CTGTGGACCTGCCAATCG and reverse, TAGCATCATTC CGCTCCTTC; HIF-1 α forward, GCAGCAACGACACAGA AACT and reverse, AGCGGTGGGTAATGGAGAC; MMP-9 forward, CCAACTACGACACCGACGAC and reverse TGGAGATGAATGGAACTGG; caspase-3 forward, AGATGG TTTGAGCCTGAGCA and reverse, CAGTGC GTATGGAG AAATGG; β -actin forward, GATGCAGAAGGAGATCAC TG and reverse, TAGTCCGCCTAGAAGCATTTG.

The specific primers and Maxima SYBR-Green/ROX qPCR Master mix were used for qPCR, with the reaction conditions as follows: 50°C pretreated for 2 min, 95°C pre-denaturing for 10 min and 95°C denaturing for 15 sec, and 60°C annealing, and extension for 60 sec for a total of 40 cycles. Triplicate wells were utilized and β -actin was used as the internal control. Quantitation was represented by cycle-threshold value (ct value). Relative mRNA value = $2^{-\Delta\text{ct}}$ ($\Delta\text{ct} = \text{Ct}_{\text{target gene}} - \text{Ct}_{\beta\text{-actin}}$). The differences between the treated and the control group were analyzed.

Statistical analysis. The data are presented as mean \pm SD, and the differences between the two groups were analyzed using χ^2 test. The differences among groups were analyzed using one-way analysis of variance test. SPSS 13.0 software (SPSS, Inc., Chicago, IL, USA) was used in the present study, and $P < 0.05$ was considered to indicate a statistically significant result.

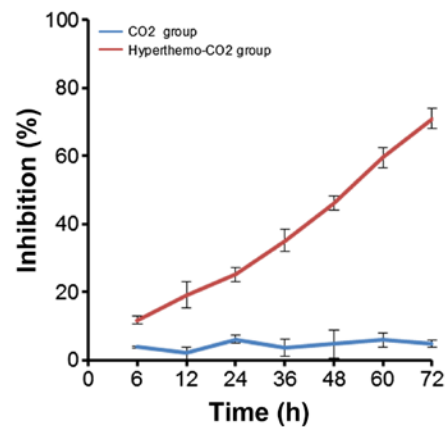


Figure 2. The inhibitory effect of each treatment on cell proliferation.

Results

Dynamic observation under a microscope on the cell proliferation and morphology. The cells from the control and CO₂ pneumoperitoneum group were attached to the wall of the Petri dish with rod-, spindle-, leave- or branch-like morphology; all were in good condition with a rapid growth rate, which reached 100% confluence within 3 or 4 days, without obvious dead cells. However, the majority of the cells from the hyperthermo-CO₂ pneumoperitoneum group started to shrink after 12 h. The cells presented with triangular or round morphology without sparapodium, the refraction of the cells increased, and the cells were detached from the wall of the Petri dish and suspended into the culture medium. The cell death and cell debris could be observed after 24 h. The total cell number was reduced and normal morphology loss aggravated with time. The dead cells and cell debris filled the whole Petri dish after 48 h (Fig. 1). The cell proliferation slowed down or arrested, and the cells recovered after 7-10 days.

Cell proliferation inhibition detection using WST-8 test. The results of WST-8 test for cell proliferation inhibition detection of each group are shown in Fig. 2. The inhibition rate was 2.00 \pm 0.62, 6.33 \pm 1.53, 4.33 \pm 1.05 and 5.00 \pm 1.14% in the CO₂ group after treatment for 12, 24, 48 and 72 h, respectively; whereas, it was 19.33 \pm 3.76, 46.33 \pm 4.86, 60.67 \pm 5.37 and 83.00 \pm 6.64% in the hyperthermo-CO₂ group. The difference between the two groups could be observed at each time point with statistical significance ($P < 0.05$), indicating that

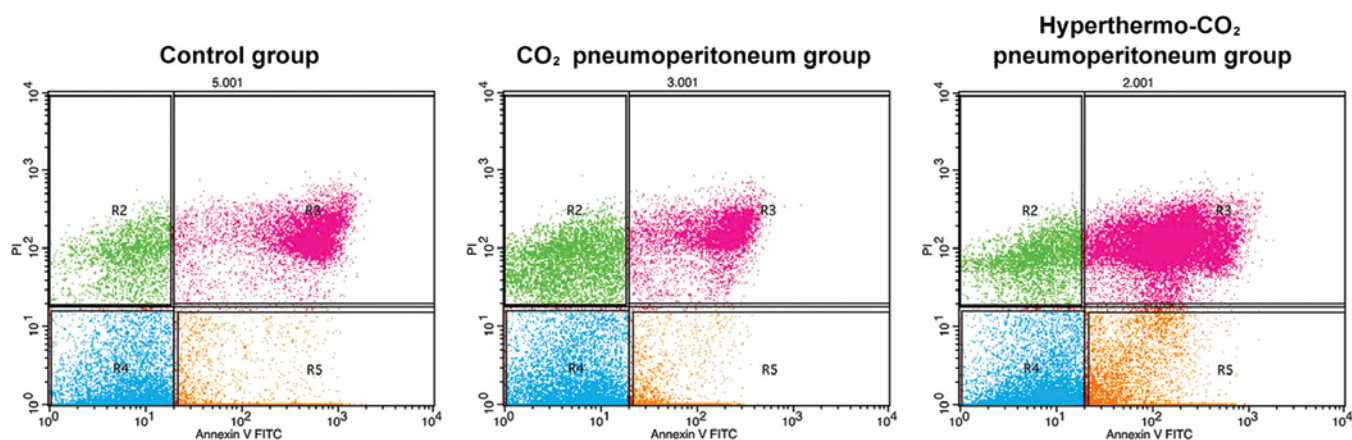


Figure 3. The scattering of cells under different treatments with Annexin V/PI staining.

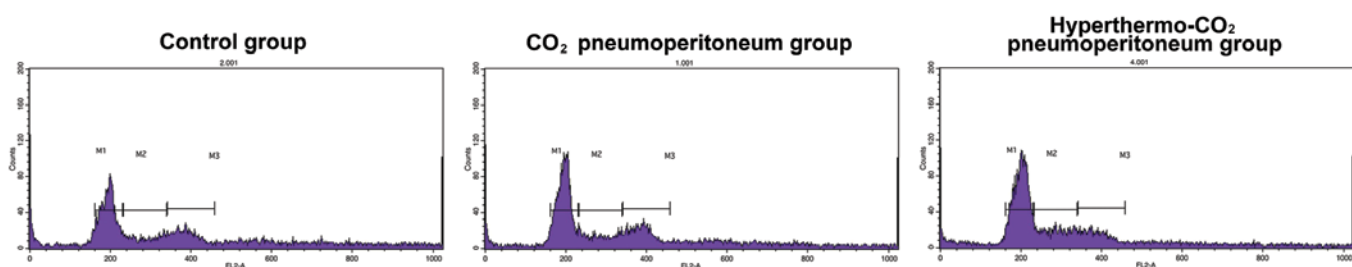


Figure 4. The effect of each treatment on the cell cycle.

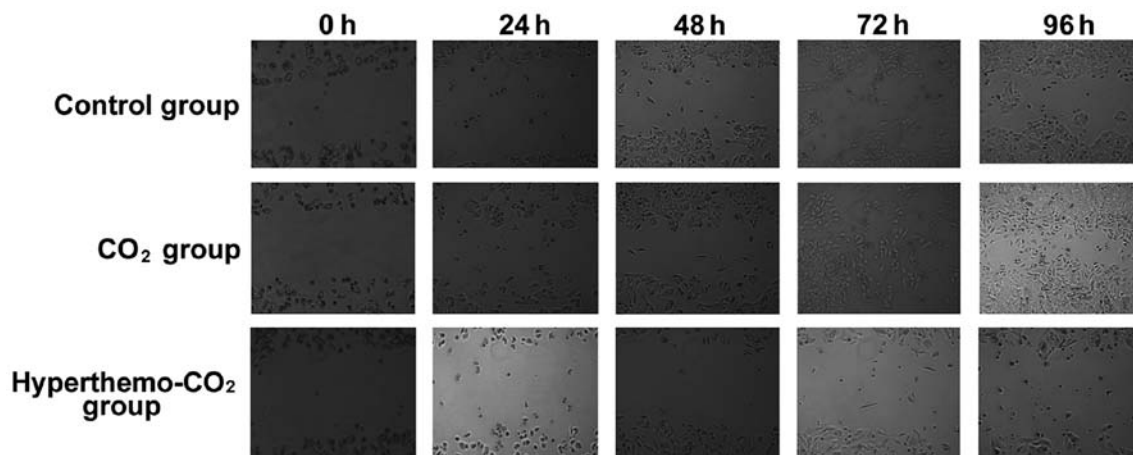


Figure 5. The effect of each treatment on the migration of cells.

CO₂ had no obvious effect on cell proliferation, while the hyperthermo-CO₂ had a significant inhibitory effect.

Cell apoptosis detection using FACS analysis. The apoptosis and necrosis of cells after treatment were analyzed using FACS with Annexin V/PI staining. The formula used for apoptosis calculation was as follows: Apoptosis rate (%) = R3 + R5. The apoptosis and necrosis rates were 11.37 ± 0.87 and $5.32 \pm 0.46\%$ in the control group, 13.26 ± 0.95 and $5.76 \pm 0.58\%$ in the CO₂ group and 45.20 ± 3.11 and $32.50 \pm 5.12\%$ in the hyperthermo-CO₂ group, respectively (Fig. 3). There was no

significant difference between the control group and the CO₂ group ($P > 0.05$), while the apoptosis and necrosis rates in the hyperthermo-CO₂ group significantly increased ($P < 0.05$), indicating that hyperthermo-CO₂ could induce apoptosis and promote necrosis of cancer cells.

Cell cycle analysis using FACS. The cell cycle was analyzed using FACS after treatment for 12 h (Fig. 4). It showed G0/G1 and S phase of $35.77 \pm 3.13\%$, and S phase of $54.17 \pm 1.64\%$ in the control, 39.37 ± 1.12 and $50.47 \pm 1.96\%$ in the CO₂, and 65.53 ± 1.75 and $19.57 \pm 1.06\%$ in the hyperthermo-CO₂ group,

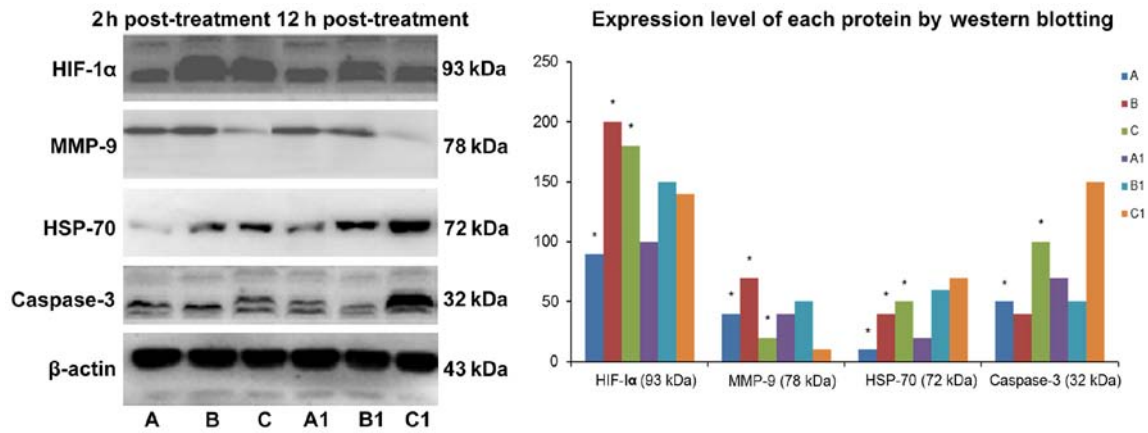


Figure 6. The expression level of proteins after each treatment. (A and A1, control group; B and B1, CO₂ group; and C and C1, hyperthermo-CO₂ group).

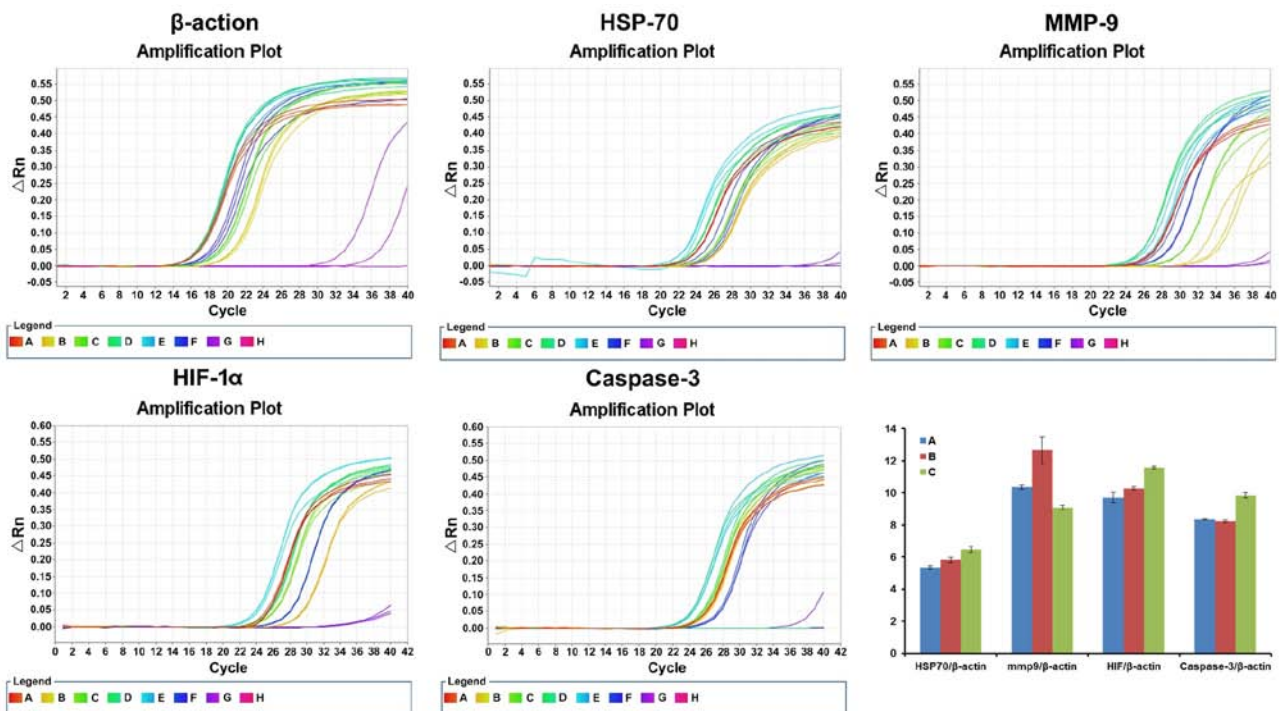


Figure 7. The effect of each treatment on the expression of genes. A, control group; B, CO₂ group; C, hyperthermo-CO₂ group.

respectively. There was no significant difference between the control and the CO₂ group ($P=0.662$), while the number of cells at G0/G1 phase increased and the number of cells at S phase decreased in the hyperthermo-CO₂ group ($P<0.05$), indicating that hyperthermo-CO₂ could arrest the cell cycle.

Extracellular fluid temperature and pH measurements. The pH value of the culture medium from the CO₂ group decreased from 7.35 to 6.12 after 30-min treatment; the temperature remained unchanged. The pH value of the culture medium from the hyperthermo-CO₂ group decreased from 7.34 to 6.20, while the temperature increased to 43°C within 5 min. The pH value of both the groups gradually returned to 7.30 after 2 h, indicating that hyperthermo-CO₂ treatment may create a transient hyperthermic, acidic and hypoxic microenvironment while the CO₂ treatment only created a transient acidic and hypoxic microenvironment.

Effect on cell migration. The migration ability of cells was tested using scratch assay (Fig. 5). The scratch gap was large with clear parallel boundaries in the three groups after scratching. The cells started to migrate into the gap after 48 h in the control group, the gap narrowed down after 72 h, and disappeared with migration of many cells into the gap. In the CO₂ group, similar observations were found. However, in the hyperthermo-CO₂ group, the gap remained large after 72 and 96 h with shrinking of the surrounding cells, apoptosis, and necrosis; the cell debris could be observed in the gap, indicating that the migration ability of cells in the hyperthermo-CO₂ group decreased.

Protein expression detection using western blotting. The results of western blotting are shown in Fig. 6. Compared with the control group, the expression level of caspase-3 protein remained unchanged, and the expression level of HSP-70,

HIF-1 α and MMP-9 proteins increased in the CO₂ group. The expression level of caspase-3, HSP-70 and HIF-1 α increased and the expression level of MMP-9 protein decreased in the hyperthermo-CO₂ group. The expression level of HSP-70 and HIF-1 α decreased whereas the expression level of caspase-3 increased after treatment for 12 h in the hyperthermo-CO₂ group, indicating that CO₂ pneumoperitoneum could enhance cell migration. Hyperthermo-CO₂ pneumoperitoneum could promote cell apoptosis and inhibit cell migration, and the effect may be reduced with time.

mRNA level detection using RT-PCR. RT-PCR result of each targeted gene 12 h after treatment is shown in Fig. 7. The relative expression of HSP-70/ β -actin in the control, CO₂ and hyperthermo-CO₂ groups was 5.34 \pm 0.09, 5.82 \pm 0.15 and 6.48 \pm 0.18, respectively. The relative expression of MMP-9/ β -actin in the control, CO₂ and hyperthermo-CO₂ groups was 10.36 \pm 0.12, 12.66 \pm 0.83 and 9.09 \pm 0.14, respectively. The relative expression of HIF-1 α / β -actin in the control, CO₂, and hyperthermo-CO₂ groups was 9.72 \pm 0.33, 10.29 \pm 0.09 and 11.56 \pm 0.09, respectively. The relative expression of caspase-3/ β -actin in the control, CO₂ and hyperthermo-CO₂ groups was 8.35 \pm 0.06, 8.23 \pm 0.08 and 9.84 \pm 0.16, respectively. Compared with the control group, the expression level of caspase-3 mRNA remained unchanged ($P=0.102$), and the expression level of HSP-70, HIF-1 α and MMP-9 mRNA increased in the CO₂ group ($P<0.05$). The mRNA level of caspase-3, HSP-70 and HIF-1 α increased, and MMP-9 mRNA decreased in the hyperthermo-CO₂ group ($P<0.05$). The findings of the present study indicated that CO₂ could increase the expression of HIF-1 α and MMP-9, which promoted the migration of cells; whereas, the hyperthermo-CO₂ increased HIF-1 α , HSP-70 and caspase-3 expression, but decreased MMP-9 expression, which promoted cell apoptosis and inhibited cell migration.

Discussion

Laparoscopic technology has rapidly developed since the first adoption in colorectal surgery, and is widely used in colorectal cancer surgeries. CO₂ is commonly used to create pneumoperitoneum, which has been a concern for some surgeons in that CO₂ pneumoperitoneum may be associated with tumor cell migration and infiltration. The potential mechanisms may include the velocity and pressure created by CO₂ pneumoperitoneum-induced tumor cell detachment and spreading (7), tumor cells seeded at the puncture site of casing pipes (8), aerosol dissemination of tumor cells by an ultrasonic knife, peritoneal acidic hypoxic microenvironment caused by CO₂ pneumoperitoneum (9), and cellular immunity alteration (10). Other researchers believed that CO₂ pneumoperitoneum had no obvious effect on tumor invasion and metastasis (1,11). It is, however, necessary to avoid any possibility of tumor invasion and metastasis caused by CO₂ pneumoperitoneum. Hyperthermia is a novel therapeutic method that increases temperature systematically or locally to the treatment temperature (42-45°C) and sustains it for a certain period to eliminate tumor cells. The major mechanism is to impair DNA repair system, denature protein, inhibit oxidative metabolism, alter microenvironment, and activate lysosomal enzymes, which eventually leads to tumor cell necrosis or apoptosis (12). In

addition, the hyperthermia alters the signaling transduction pathways or networks of cells, leading to impaired cell cycle and DNA replication checkpoint and activation of transcription factors responsible for tumor cell apoptosis (13-16). CO₂ gas is a carrier with good heat conduction and dispersion, which could conduct heat rapidly within the abdominal cavity. In the present study, CO₂ was heated to 43°C, which is the hyperthermia temperature, and the pressure of 14 mmHg was maintained for 2 h, which also simulates a laparoscopic operation. This setting may be able to inhibit tumor cell migration and eliminate the aerosol disseminated tumor cells in the first place during the laparoscopic operations, which was expected to prevent or reduce the invasion and metastasis of tumor cells by CO₂ pneumoperitoneum.

The present study showed that CO₂ pneumoperitoneum had no obvious effect on cell morphology, proliferation or necrosis; however, the hyperthermo-CO₂ pneumoperitoneum led to cell shrinking, reduced proliferation or growth arrest, apoptosis or necrosis. The proliferation inhibition rate and the apoptosis rate were 5% and 3.26 \pm 0.95% by CO₂ pneumoperitoneum, respectively; and they were >40% and 45.20 \pm 3.11% by hyperthermo-CO₂ pneumoperitoneum, respectively. There was no effect of CO₂ pneumoperitoneum on the cell cycle, while the cell cycle was arrested by hyperthermo-CO₂ pneumoperitoneum. These findings indicated that CO₂ pneumoperitoneum may not affect cell growth, proliferation and apoptosis; whereas, hyperthermo-CO₂ pneumoperitoneum was able to inhibit cell growth and proliferation and promote cell apoptosis. Heat shock protein (HSP) is a heat-induced adaptive protein. HSP could be produced when the cells were exposed to external stimuli such as heat, radiation and chemotherapy. HSP-70 is a member of the HSP family, which is involved in protein synthesis, processing, folding and transport, and related to the occurrence, development, immunity, drug resistance and prognosis of the tumor (17). The hyperthermo-CO₂ pneumoperitoneum was shown to upregulate the expression of HSP-70 mRNA and protein in the present study, and the increased level of HSP-70 promoted tumor cell apoptosis and inhibited tumor cell metastasis. Caspase family plays an important role in cell apoptosis. Caspase-3 is the key member and plays multiple roles in the signaling pathways of apoptosis. Caspase-3 exists in cytoplasm as zymogen and is activated in the early stage of apoptosis to degrade the substrates in cytoplasm and nuclei, eventually leading to apoptosis (18). Western blotting and RT-PCR showed that caspase-3 gene and protein both increased after hyperthermo-CO₂ treatment in the present study. The hyperthermo-CO₂ pneumoperitoneum in the present study may be able to enhance caspase-3 activation in tumor cells through heat damage, acidosis and hypoxia, and finally initiate apoptosis. In contrast, CO₂ treatment had no obvious effect on caspase-3 at either gene or protein level, implying that CO₂ treatment may not have a significant effect on tumor cell apoptosis.

The migration ability of tumor cells is one of the important factors for metastasis. Our findings of cell scratch assay indicated that CO₂ pneumoperitoneum could increase the migration of tumor cells while the hyperthermo-CO₂ pneumoperitoneum inhibited migration. Hypoxia-inducible factor-1 α (HIF-1 α) was reported to regulate the transcription of a number of regulatory factors to elicit adaptive responses

to hypoxia, maintaining high energy metabolism of tumor cells, inducing angiogenesis, promoting tumor invasion and metastasis, and resulting in drug resistance (19). Both CO₂ pneumoperitoneum and hyperthermo-CO₂ pneumoperitoneum could create hypoxia microenvironment and increase HIF-1 α expression at both gene and protein levels, which was confirmed in the present study by western blotting and RT-PCR. CO₂ pneumoperitoneum was shown to promote tumor cell migration; however, hyperthermo-CO₂ pneumoperitoneum could directly adversely affect tumor cells by heat damage. Matrix metalloproteinase-9 (MMP-9) is a type of zinc ion-dependent endopeptidase degrading extracellular matrix (ECM) and playing a key role in tumor invasion and metastasis. MMP-9 is considered a marker of tumor invasion and metastasis (20). In the present study, western blotting and RT-PCR showed that the expression of MMP-9 increased by CO₂ pneumoperitoneum; however, it decreased by hyperthermo-CO₂ pneumoperitoneum, indicating that CO₂ pneumoperitoneum could promote invasion and migration of tumor cells by upregulating MMP-9 while hyperthermo-CO₂ pneumoperitoneum inhibited invasion and migration of tumor cells by downregulating MMP-9.

Hence, CO₂ pneumoperitoneum may not have an obvious effect on the proliferation and apoptosis of colon cancer cells, but could enhance the migration ability by upregulating HIF-1 α and MMP-9 expression by creating acidic hypoxic microenvironment. However, hyperthermo-CO₂ pneumoperitoneum could inhibit growth, proliferation and migration of colon cancer cells by upregulating HSP-70, HIF-1 α and caspase-3 expression and downregulating MMP-9 expression by creating hyperthermic acidic hypoxic microenvironment. Hyperthermo-CO₂ pneumoperitoneum could convert the CO₂-induced promotion effect on cell migration. Since the present study was an *in vitro* assay based on a tumor cell line, the effect of hyperthermo-CO₂ pneumoperitoneum on normal peritoneal cells should be investigated. Animal as well as clinical studies are also needed to further confirm the findings of the present study.

Acknowledgements

The present study was supported by funding from the Shanghai Municipal Commission of Health and Family Planning (20134260).

References

- Bloomston M, Kaufman H, Winston J, Arnold M and Martin E: Surgical management of colorectal cancer in the laparoscopic era: A review of prospective randomized trials. *J Natl Compr Canc Netw* 3: 517-524, 2005.
- Bing F and Hong Z: The effect of CO₂ pneumoperitoneum on the growth and metastasis of malignant tumors of the rectum. *J Exp Sur* 22: 1021, 2005.
- Jingli C, Rong C and Rubai X: Influence of colorectal laparoscopic surgery on dissemination and seeding of tumor cells. *Surg Endosc* 20: 1759-1761, 2006.
- Hohenberger W, Schneider C, Reymond MA, Scheidbach H and Köckerling F: Laparoscopic resection of colorectal malignancy - an oncological risk? *Zentralbl Chir* 122: 1127-1133, 1997 (In German).
- Al-Shammaa HA, Li Y and Yonemura Y: Current status and future strategies of cytoreductive surgery plus intraperitoneal hyperthermic chemotherapy for peritoneal carcinomatosis. *World J Gastroenterol* 14: 1159-1166, 2008.
- Zhenggang Z: Comprehensive treatment and issues related to gastric cancer recurrence. *Chin J Sur* 25: 181-183, 2005.
- Gutt CN, Kim ZG, Hollander D, Bruttel T and Lorenz M: CO₂ environment influences the growth of cultured human cancer cells dependent on insufflation pressure. *Surg Endosc* 15: 314-318, 2001.
- Ceccarelli G, Casciola L, Nati S, Bartoli A, Spaziani A, Stefanoni M, Conti D, Fettucciari V, Di Zitti L, Valeri R, *et al*: Neoplastic residues in the trocar tract in oncologic laparoscopic surgery. *Minerva Chir* 59: 243-248, 2004 (In Italian).
- Wittich P, Steyerberg EW, Simons SH, Marquet RL and Bonjer HJ: Intraperitoneal tumor growth is influenced by pressure of carbon dioxide pneumoperitoneum. *Surg Endosc* 14: 817-819, 2000.
- Novitsky YW, Czerniach DR, Kaban GK, Bergner A, Gallagher KA, Perugini RA and Litwin DE: Immunologic effects of hand-assisted surgery on peritoneal macrophages: Comparison to open and standard laparoscopic approaches. *Surgery* 139: 39-45, 2006.
- Hao YX, Zhong H, Zhang C, Zeng DZ, Shi Y, Tang B and Yu PW: Effects of simulated carbon dioxide and helium pneumoperitoneum on proliferation and apoptosis of gastric cancer cells. *World J Gastroenterol* 14: 2241-2245, 2008.
- Van der Speeten K, Stuart OA and Sugarbaker PH: Using pharmacologic data to plan clinical treatments for patients with peritoneal surface malignancy. *Curr Drug Discov Technol* 6: 72-81, 2009.
- Zhang XL, Hu AB, Cui SZ and Wei HB: Thermotherapy enhances oxaliplatin-induced cytotoxicity in human colon carcinoma cells. *World J Gastroenterol* 18: 646-653, 2012.
- Tabuchi Y, Wada S, Furusawa Y, Ohtsuka K and Kondo T: Gene networks related to the cell death elicited by hyperthermia in human oral squamous cell carcinoma HSC-3 cells. *Int J Mol Med* 29: 380-386, 2012.
- Jung HJ and Seo YR: Protective effects of thioredoxin-mediated p53 activation in response to mild hyperthermia. *Oncol Rep* 27: 650-656, 2012.
- Sturm I, Rau B, Schlag PM, Wust P, Hildebrandt B, Riess H, Hauptmann S, Dörken B and Daniel PT: Genetic dissection of apoptosis and cell cycle control in response of colorectal cancer treated with preoperative radiochemotherapy. *BMC Cancer* 6: 124, 2006.
- Ito A, Shinkai M, Honda H, Yoshikawa K, Saga S, Wakabayashi T, Yoshida J and Kobayashi T: Heat shock protein 70 expression induces antitumor immunity during intracellular hyperthermia using magnetite nanoparticles. *Cancer Immunol Immunother* 52: 80-88, 2003.
- Depraetere V and Golstein P: Dismantling in cell death: Molecular mechanisms and relationship to caspase activation. *Scand J Immunol* 47: 523-531, 1998.
- Zhu H, Feng Y, Zhang J, Zhou X, Hao B, Zhang G and Shi R: Inhibition of hypoxia inducible factor 1 α expression suppresses the progression of esophageal squamous cell carcinoma. *Cancer Biol Ther* 11: 981-987, 2011.
- Liu D, Guo H, Li Y, Xu X, Yang K and Bai Y: Association between polymorphisms in the promoter regions of matrix metalloproteinases (MMPs) and risk of cancer metastasis: A meta-analysis. *PLoS One* 7: e31251, 2012.